Electrical Measurement of Cell-to-Cell Variation of Critical Charge in SRAM and Sensitivity to Single-Event Upsets by Low-Energy Protons

James M. Cannon, *Student Member, IEEE*, T. Daniel Loveless, *Senior Member, IEEE*, Rafael Estrada, Ryan Boggs, S. P. Lawrence, Gabriel Santos, Michael W. McCurdy, *Senior Member, IEEE*, Andrew L. Sternberg, Donald R. Reising, *Senior Member, IEEE*, Thomas Finzell, and Ann Cannon

***Abstract*—The distribution of single-event upsets (SEUs) in commercial-off-the-shelf (COTS) static random access memory (SRAM) has generally been thought to be uniform in a device. However, process induced variation within a device gives rise to variation within the cell level electrical characteristic known as the data retention voltage (V_{DR}). Furthermore, V_{DR} has been shown to directly influence the critical charge (Q_C) necessary for stored data to upset. Low-energy proton irradiation of COTS SRAMs exhibits a preference toward upsetting cells with lower Q_C. An electrical procedure is presented to map relative cell critical charge values without knowledge of the underlying circuitry, allowing customized device usage. Given cell level Q_C knowledge, a device can have its cells "screened" such that those with low Q_C are not used to store data. This work presents the results such a screening process has on the SEU per bit cross-section.**

***Index Terms*—Proton Radiation Effects, Radiation Hardness Assurance, Single Event Upsets, Static Random Access Memory**

I. Introduction

Single event radiation effects are a significant concern for highly scaled and commercial-off-the-shelf (COTS) microelectronics technologies. Static-Random-Access-Memories (SRAM) represent a ubiquitous class of integrated circuits that utilize dense arrays of memory cells for satisfying increasing demands for low power, mass, and cost, especially in small spacecraft systems [1]–[4]. However, COTS SRAMs are highly susceptible to single-event upsets (SEUs) due to their low critical charge (Q_C) levels and dense cell architectures. SEU test results for unhardened SRAMs fabricated in highly scaled technologies indicate that the memory cells can be susceptible to upset by direct ionization by protons with linear energy transfer (LET) values less than 1 MeV-cm^2/mg [5], [6]. These low-LET thresholds and sensitivity to upsets by protons with energies less than 2 MeV are problematic for COTS-based spacecraft architectures, such as CubeSats, because they can result in insurmountable bit error rates [6].

Moreover, highly scaled CMOS technologies are increasingly susceptible to issues related to manufacturing process variability. The innate variation in process parameters gives rise to intra-die inter-die feature differences that have consequences for SEU hardness assurance [7]–[16]. In [7], Massengill, *et al.*, suggested that non-ideal cross-section curves can partially be explained by distributions of SRAM critical charge (Q_C). Since, many works have discussed the impacts of process variability on radiation effects models [9], SRAM electrical parameters [10], [15], [16], and soft error rates (SER) [8], [11]–[14], [17]. In [18] and [19], process-induced variability was identified as the primary source of variation of the LET threshold, resulting in measured cross-section values several orders of magnitude lower than physical device feature sizes. Torrens, *et al.*, showed in [17] that such impact can be measured electrically (without the need for radiation testing) by characterizing the word-line voltage margin. Torrens' technique can estimate the SER following a calibration of a small number of parts with radiation data, and requires minor changes to the SRAM peripheral components. Kobayashi, *et al.*, further suggested that the data retention voltage (V_{DR}) can likewise be used to predict SEU critical charge, and suggested V_{DR} as an empirical fitting parameter for cross-section estimates [15], [16].

In this work, an electrical measurement technique is proposed for characterization of each individual cell's Q_C in an arbitrary SRAM, without the need to modify existing circuitry. The proposed technique requires the measurement of cell V_{DR} values through modification of the holding voltage

Manuscript received October 2, 2020; revised January 1, 2021 and January 27, 2021; accepted February 15, 2021. Date of current version is February 21, 2021. This work was supported in part by the National Science Foundation (NSF) Research Experience for Undergraduates (REU) Program, #1757777. *Corresponding authors: James Cannon; T. Daniel Loveless.*

J. M. Cannon was with the Department of Electrical Engineering, University of Tennessee at Chattanooga, Chattanooga, TN 37403 USA and also with the Department of Physics and Astronomy, Macalester College, St. Paul, MN 55105 USA. He is now with the Department of Aerospace Engineering Sciences, University of Colorado Boulder, Boulder, CO 80303 USA (e-mail:James.Cannon-1@Colorado.edu).

T. D. Loveless, S. P. Lawrence, G. Santos, and D. R. Reising are with the Department of Electrical Engineering, University of Tennesee at Chattanooga, Chattanooga, TN 37403.(e-mail: Daniel-Loveless@utc.edu)

R. Estrada was with the Department of Electrical Engineering, University of Tennessee at Chattanooga, Chattanooga, TN 37403 USA. He is now with the Department of Electrical Engineering, New Mexico Institute of Mining and Technology, Socorro, NM 87801 USA.

R. Boggs was with the Department of Electrical Engineering, University of Tennessee at Chattanooga, Chattanooga, TN 37403 USA. He is now with NASA GSFC, Greenbelt, MD 20771 USA.

M. W. McCurdy and A. L. Sternberg are with the Depatment of Electrcial Engineering and Computer Science, Vanderbilt University, Nashvile, TN 37240 USA.

T. Finzell was with the Department of Physics and Astronomy, Macalester College, St. Paul MN 55105 USA. He is now with the Department of Computational Mathematics, Science and Engineering, Michigan State University, East Lansing, MI 48824 USA.

A. Cannon is with the Department of Mathematics and Statistics, Cornell College, Mt. Vernon IA 52314

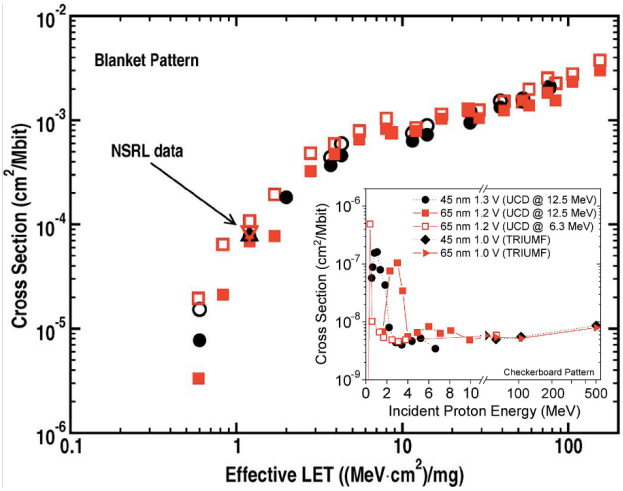

Fig. 1: Heavy-ion (Texas A&M and NASA Space Radiation Laboratory at Brookhaven), and (inset) proton upset cross sections for 45 and 65 nm SOI SRAMs (from [5]).

(V_{Hold}), and results in device-wide logical mapping of relative cell Q_C values. Low-energy proton irradiation and electrical experiments of COTS SRAM devices are used to show that the upset cross-sections near and below the average LET threshold are preferentially caused by nominally weak SRAM cells. Characterization shows that the weak cells can be determined through an electrical screening process before device use; as a result, the error rate may be limited through a device-specific selection of memory cells.

II. Background

Since protons with less than 2 MeV of kinetic energy were seen to result in SEUs in 65 nm SRAMs [20], the impacts of low-energy protons, the need for improved hardness assurance, and the importance of such vulnerability to system-level SEU performance have all been studied extensively [5], [6], [21]–[27]. As discussed in [5] and shown in Fig. 1, highly scaled SRAMs exhibit a spreading of measured cross-sections at low and high LET values. Consequently, some devices have no clear LET threshold or saturated cross-section. The spread in the estimated LET threshold, including sensitivity to low-energy protons, is partially explainable by manufacturing-induced process variation resulting in a spreading of SRAM cell Q_C values [19]. In contrast, the increased cross-sections at high LET are explainable as multiple bit upsets [5]. This behavior has subsequently been observed to worsen in smaller geometry SRAMs [6] and is particularly problematic for applications dominated by low-LET ions and low-energy protons. This work presents a methodology for measuring the relative Q_C values for each cell within an SRAM through a purely electrical characterization, without the need for radiation testing. The technique leverages the influence of inherent process-induced variability, including spatially dependent lithography-induced changes in feature size and random threshold voltage assignment due to dopant fluctuations [28], on the behavior of a specific SRAM. These characteristics have been shown useful in creating run-time cryptographic keys and physically unclonable functions (PUFs) for data security purposes [28].

An empirical mapping of the spatial variations in relative Q_C values in SRAMs is performed. Thus, it is possible to map the cells within an SRAM that will be nominally sensitive to LET values below the average LET threshold for the device (i.e., "weak" cells). Results from irradiation with 1.8 MeV protons show that a disproportionate amount of SEUs in the SRAM are due to the weak cells, rather than a representative sensitive volume within all SRAM cells. This work shows that, therefore, it is possible to characterize the impact of process variability on radiation vulnerability through a pre-irradiation electrical test. It may further be possible to reduce the SEU cross-sections at low LET values and low proton energies by limiting the use of the nominal weak cells in an application.

III. Electrical Characterization

Electrical characterization of each COTS SRAM was performed using a custom memory tester comprised of a Texas Instrument (TI) MSP430F2618 16-bit microcontroller unit (MCU) and an Analog Devices AD5235 1024-position digital potentiometer. This memory tester was used to vary V_{Hold}, the supply voltage (V_{DD}) when data is being held, to COTS SRAM devices at a resolution of 2 mV. Hexadecimal data patterns of 0x00 (all zeros), 0xFF (all ones), 0xAA (checkerboard), and 0x55 (checkerboard) were written to the device. Following data writing, V_{Hold} was reduced from the manufacturers recommended retention voltage in increments of 2 mV and held for two seconds. An on-board analog to digital converter (ADC) sampled the voltage after 1 second and this value was recorded as V_{Hold}. After the two-second hold time, the supply voltage was raised back to the nominal value, and each byte within the SRAM was read. Any discrepancy from the original data pattern was caught, and the logical addresses of the failed cells recorded. This process was repeated until at least 50% of the SRAM cells reported failure, beyond which the failure pattern resembles the random distribution associated with the SRAM power cycle and represents the SRAM's PUF [28]. Complete characterization requires approximately 20 minutes per kByte,

Several commercially available SRAM devices were analyzed, including the 256 kByte MicroChip 23k256 in both Dual Inline Packages (DIP) and Thin Shrink Small Outline Packages (TSSOP), and the 256 kByte On Semiconductor N25S830HA in TSSOP. Data from 7 MicroChip SRAMs (labeled as AD01, AD02, AD03, AT01, AT02, RD03, and RD04) and one On Semiconductor SRAM (labeled as BT01) are reported. The prefix "A" designates a Microchip device, "R" designates a de-lidded device used in radiation experiments, while the prefix "B" designates an On Semiconductor device. The second character "D" corresponds to lidded DIP devices while "T" correspond to lidded TSSOP devices. The nominal supply voltage for all devices under test (DUTs) is 3.3 V, and the manufacturer's recommended minimum V_{Hold} is 1.2 V. However, no devices reported upsetting cells for applied holding voltages of 0.5 V or greater. Fig. 2 shows the percentage of total cells reporting data retention failure versus

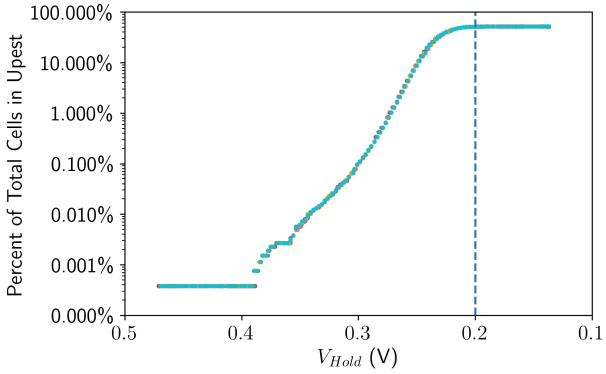

Fig. 2: The percent of total cells reporting data retention failure versus the holding voltage (V_{Hold}) for DUT AT01 for 10 distinct trials plotted on top of each other
. The approximate saturation of cells in upset is noted by the blue dashed line at 0.2 V

V_{Hold} for AT01 across 10 trials. The exact overlap of all 10 trials when plotted this way shows this measurement technique is highly repeatable. This plot makes it clear that the saturation of failed cells (greater than 50% of cells indicating failure) occurred at a V_{Hold} of approximately 0.2 V. Each DUT was characterized for holding voltages at least as low as 0.21 V.

To gain insights into the device-wide behavior, visualizations of the cells in upset were made. Every bit's logical address was mapped 1-to-1 to a specific pixel in a 512x512 image. Importantly, a cell location to logical address for these commercial devices is unknown meaning any spatial features present in our imaging may or may not be real. Fig. 3 illustrates an example spatial map of cell failures where each white pixel represents one failed cell in DUT RD03 when electrically set to a V_{Hold} of 0.249V. Also shown in the

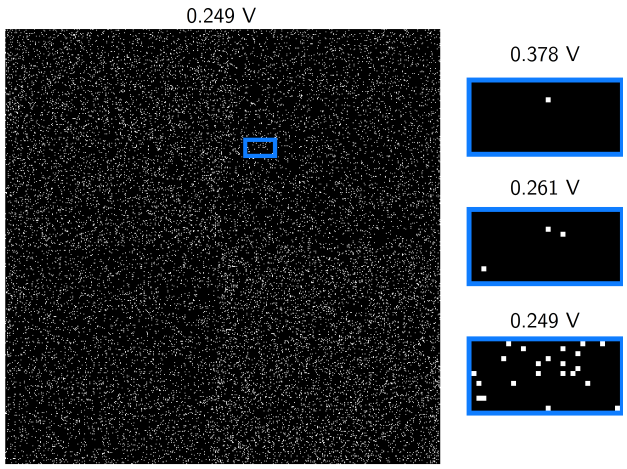

Fig. 3: A virtual spatial map of the failed cells for an SRAM device (AD01) at V_{Hold} = 0.249 V. White pixels represents upset cells while black pixels are cells that retained their data. A subset of cells at V_{Hold} values from 0.378 V to 0.249 V is also shown, illustrating that the same cells are seen to upset consistently once a threshold holding voltage is reached.

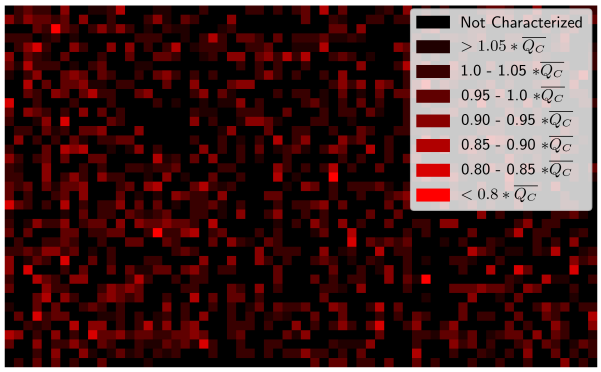

Fig. 4: A virtual spatial heat map of Q_C to upset for a subset of the cells in DUT RD03. Brighter red pixels have a lower relative Q_C. Black cells did not upset.

figure is a subset of cells for RD03 at various V_{Hold} values, illustrating the onset for upset for multiple cells. These data show a high level of consistency with the same cell upsetting at subsequently lower V_{Hold} values, after having been re-initialized. This consistency is observed across multiple trials, indicating that every cell has a unique minimum V_{Hold} below which it will upset. Said another way, every cell has a voltage value (V_{DR}) that indicates the minimum data retention voltage for that cell.

IV. Data Retention Voltage to Critical Charge to Upset

In [16], Koybayashi *et. al* (citing [15], [29]) discusses how Q_C can be effectively estimated via the data retention voltage, V_{DR}, using

$$Q_c = aC(V_{DD} - V_{DR}) \tag{1}$$

where a is a constant and C is the load capacitance [15], [16], [29]. Importantly, a is a constant on the device-level and is immune to variations in either Q_C and V_{DR} [29]. V_{DR} is the minimum voltage a cell needs to retain the data written to it. If data is written to a cell and V_{DD} is lowered below V_{DR}, that cell will upset. Thus, cells with lower than the average minimum holding voltages have larger Q_c than average. Likewise, the "weakest" cells, those with the highest minimum holding voltages, exhibit the lowest Q_c levels. This relationship is due to the inverse dependence of the cell's minimum holding voltage on the capacitive energy storage. Given cell V_{DR} values, those cells can be assigned a relative Q_C value allowing the cells to be compared against each other and aggregate SRAM variability statistics to be examined.

An example of the spatial mapping of Q_C for the DUT RD03 is shown in Fig. 4. The bright red pixels represent cells with a lower Q_C relative to the device's average. This image shows a spread of Q_C from less than 80% of the device mean critical charge to upset ($\overline{Q_C}$) to over 105% of $\overline{Q_C}$ The black pixels represent cells that did not exhibit data retention failure.

Fig. 5 shows histograms of Q_C for all cells within all DUTs. The distributions are normalized such that $\overline{Q_C}$ has a value of

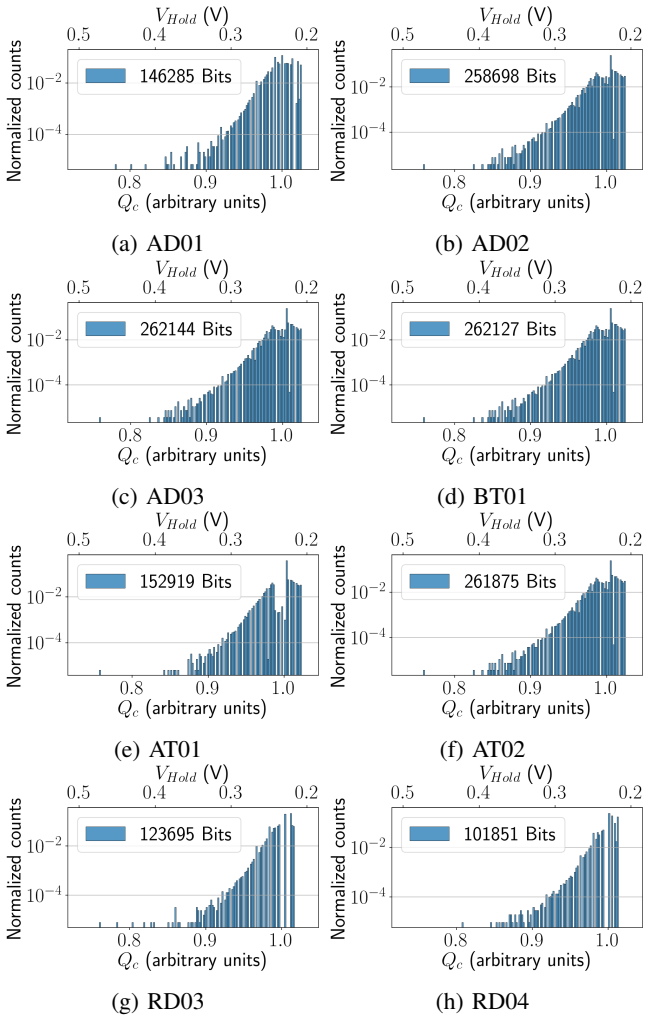

Fig. 5: The PMFs of Q_C for all cells electrically characterized in all DUTs. The lower horizontal axis shows relative Q_C values while the upper horizontal axis shows the corresponding V_{DR} value.

one, and the sum of all bins totals one, representing a probability mass function (PMF). This non-Gaussian distribution has a prominent left skew with a tail extending to nearly -25% of the mean, matching previous V_{DR} predictions [29]. Across the different manufacturers and package types examined, these data show consistency in general shape. In most cases, not every cell upsets and thus not every cell can be assigned a relative Q_C. However, examining (c) shows that all 262,144 cells upset indicating that the shape of these PMFs are not a result of systematic bias in the test. Sub-figures (g) and (h) show the baseline PMFs of Q_C for the irradiated devices (RD03 and RD04) discussed in Section V.

V. Radiation Characterization

Two de-lidded MicroChip 23k256 DIP devices (RD03 and RD04) were irradiated at the Vanderbilt University Pelletron with 1.8 MeV protons, corresponding to an approximate LET of 0.12 MeVcm^2/mg at the surface of the DUT. Before radiation exposure, each DUT was characterized using the

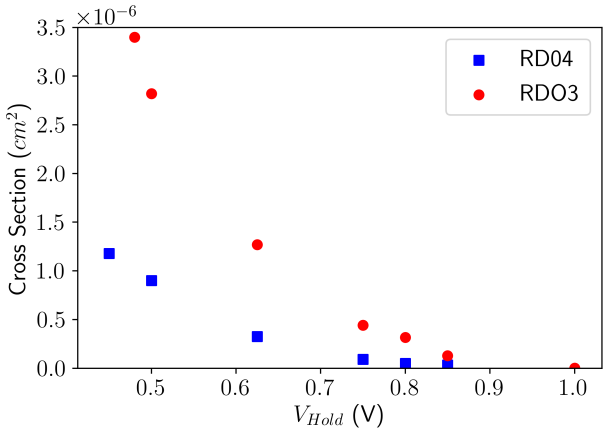

Fig. 6: Measured SEU cross-sections (cm^2) for 2 MicroChip 23k256 SRAMs as a function of holding voltage (V) for 1.8 MeV protons.

methodology discussed in the previous section, for V_{Hold} values between 0.607 V and 0.217 V. During radiation exposure, the V_{Hold} of the DUT was lowered to adjust the Q_C values until SEUs were observed. Each DUT was maintained at a V_{Hold} value greater than the highest characterized V_{DR} for that device to ensure that the applied V_{Hold} value did not result in random bit flips. As shown in Fig. 5, DUT RD03 has a maximum V_{DR} of 0.472 V, with exactly one cell recording failure. Correspondingly, RDO3 was never irradiated with V_{Hold} lower than 0.483 V. Likewise, RD04 has a maximum V_{DR} of 0.423 V and thus V_{Hold} was kept above 0.455 V.

As expected, the DUT cross-sections increase with decreasing holding voltage, as seen in Fig. 6, where the average SEU cross-sections versus holding voltage are plotted for devices RD03 (red circles) and RD04 (blue squares). Interestingly, these two identical devices have significantly different cross-section behavior. RD03 has consistently higher measured cross-sectional area than RD04. Examining Fig. 5 (g) and (h) shows that RD03 has a larger tail skewed toward low Q_C. It may, then, be possible to use this electrical test to compare otherwise identical devices. Data were taken at a variety of exposure times and for holding voltages between 1.0 V and 0.45 V. After each test, the address of each upset bit was logged.

DUT RD03 was irradiated a total of 33 separate times and RD04 was irradiated 31 separate times. The total fluence of each trial ranged from 2.0×10^7 protons for a 5 second exposure to 1.2×10^9 protons for a 300 second exposure. After irradiation, DUT RD03 had a Total Ionizing Dose (TID) of 14.9 krads(SiO_2) and DUT RD04 had a TID of 15.4 krads(SiO_2). Following irradiation, the DUTs' functionality were verified to ensure that TID did not bias the results.

Following each proton exposure, the distribution of Q_C values (identified via electrical characterization) for the cells reporting SEUs was compared to the distribution of Q_C for the entire SRAM. An example of this is shown in Fig. 7 for RD03. For each radiation exposure, the mean Q_C value of the cells reporting SEUs was compared to the mean of the

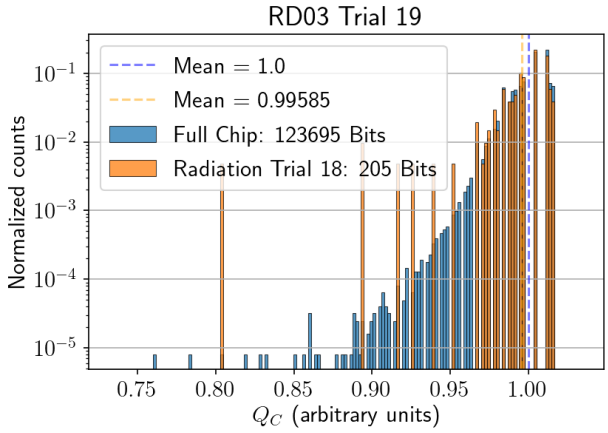

Fig. 7: Example post-irradiation distribution of Q_C of cells reporting SEUs when irradiated (orange) superimposed on top of the distribution of the full device (RD03) Q_C values (blue).

distribution from the full device. In the example shown in Fig. 7, the orange PMF shows proportionately more cells at lower Q_C upsetting than the PMF of the full device. Beyond a visual inspection, this is captured concisely by comparing the means of both distributions. Cells that reported SEUs but did not have an electrically characterized Q_C were not included in the analysis.

Fig. 8 shows two histograms of the mean values of Q_C for cells reporting SEUs during all trials for both devices (RD03 and RD04). The average Q_C of 1 for each DUT is also shown as a solid line. There is a significant skew toward lower values of Q_C to upset in the cells that upset during these trials.

For DUT RD03, 29 out of 33 radiaion exposures had mean relative (Q_C) values lower than the device mean. Because the data were skewed and therefore non-Gaussian, the typical *t*-test for a mean was not appropriate. Instead, a randomization test for a mean using 100,000 randomization samples on these data was conducted. A null hypothesis of a true mean equal to 1 was used for the test. For RD03, the p-value was reported to be 7.0E-5, giving extremely strong evidence to reject the null hypothesis. This indicates that there is statistically significant evidence that the mean Q_C for cells reporting SEUs during proton irradiation is below the DUT mean Q_C. In other words, the distribution of cells upsetting when struck by low-energy protons in this device skews towards cells identifiable as "weak" via the electrical characterization presented in Section III.

DUT RD04 had 24 out of 31 radiation exposures with mean Q_C values below the device mean. Conducting the same statistical test for the data as described above, gives a p-value of 3.3E-3. This value is statistically significant well beyond a typical 0.05 p-value threshold and indicate that it is extremely unlikely that these means would be reported in the case that the true mean of irradiated cells is equal to the electrically characterized mean of the full device. Said another way, SEUs for both devices exhibited a statistically significant and consistent favoring of cells with lower Q_C than the mean of the device. For a 1.8 MeV proton, nominally "weak" cells have a more than random chance of upsetting and thus can be screened out electrically.

VI. Impacts of Q_C Variation on SEU Response

Given the significant evidence for weak cells that can be electrically identified to be more likely to upset when exposed to low-LET radiation, some possible applications are considered.

A. SEU Mitigation

First, it may be possible to mitigate SEU at low-LET values, thus increasing the relative LET threshold through the

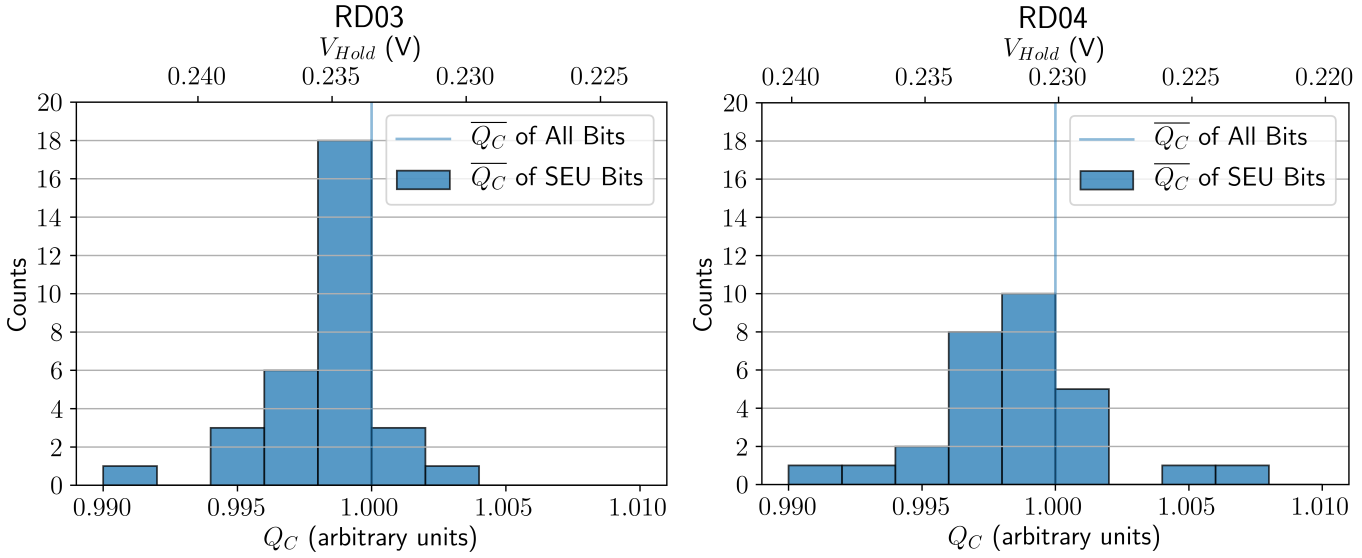

Fig. 8: Histograms showing the distribution of the mean values of Q_C for cells reporting SEUs during all radiation trials for both MicroChip SRAM DUTs (left-RD03 and right-RD04). The average Q_C for each DUT is also shown as a solid line. These distributions show a clear bias of electrically identifiable weak cells toward upsetting when irradiated.

application of a 'virtual screening process'. To illustrate, the data used to calculate the σ_{SEU}/bit were modified. Screening thresholds were set at various Q_C values from $0.970 * \overline{Q_C}$ to $1.012 * \overline{Q_C}$. Cells with Q_C values lower than the screening threshold were discounted as upset events and also removed from the total population of cells. This leads to (2)

$$\sigma_{SEU/\text{Bit}} = \frac{N - N_T}{F * (C - C_T)} \tag{2}$$

where N is the number of upsets, N_T is the number of cells that upset with Q_C below the chosen threshold, F is the particle flux (particles per area), C is the number of cells of the device, and C_T is the total number of cells with Q_C below the chosen threshold.

The first screen applied was to simply remove all cells for which there was no electrical characterization. Applying this baseline screening results in a σ_{SEU}/bit that is similar to the original, though consistently higher. The slight increase in σ_{SEU}/bit following the baseline screening of RD03 and RD04 results from incomplete electrical characterization of V_{DR}. RD03 and RD04 were only characterized for V_{Hold} values down to 0.217 V, or approximately $1.02 * \overline{Q_C}$. This is quite close to the 50% saturation level noted at 0.2 V in Fig. 2, but below the knee of the curve. As a result, these data are further left skewed than is truly representative. This means that it is likely that the characterized cells as a group are "weaker" than the true average of the device. So, when only the characterized cells are considered, the cross-section—which represents a probability of upset—increases. Then, to evaluate whether any further screening is effective at reducing the cross-section, the cross-section per bit of the *characterized* cells will be used as the baseline.

Fifteen threshold Q_C values were chosen for both RD03 and RD04. For each threshold, the ratio of the screened per bit cross-section divided by the baseline was calculated for each of the 32 and 28 radiation trials respectively. Each of these were then converted into a percent change. Fig. 10 shows two plots of how each of the first eight different threshold values affects the cross-section for RD03 and RD04 respectively. Each screen was applied to the data from all radiation trials for both devices (32 and 28 trials respectively). The results form distributions of responses for each particular screening value which are shown as boxplots. The median values are noted as solid orange lines. As is normal for boxplots, the box represents the interquartile range which encompasses the middle 50% data. Outliers are noted with diamonds. This plot is enlarged to show detail when a small fraction of cells are screened out. Consider the 7$^{\text{th}}$ boxplot on the left plot of Fig. 10. In this boxplot, 15% of the "weakest" cells have been screened out. The median response across all 32 trials is a reduction of the cross section by 4%. For that same screening threshold, the interquartile range shows that 50% of the trials had their cross section reduced by between approximately 2% and 7%. Two trials in this example were statistical outliers. These trials had much greater change in their cross section than the majority of the trials and saw -35% and -41% change noted as the diamonds.

B. Variability Analysis

Electrical screening of "weak" cells within an SRAM appears to only moderately impact the σ_{SEU}/bit, though analysis with various LET values is required to further understand potential applications in SEU mitigation. On average, this technique produces a lower cross section than is typical of the aggregate device, but the percent change is disproportionate when compared to the percent of cells required to be screened out. A possible extension of this analysis would be to compare the efficacy of this technique to current error correcting codes (ECC), or to use the reported cell maps to develop variability-aware ECC.

The process presented herein may also be useful for pre-irradiation intra- and inter-device variability analyses. While this study lacked a large number of parts to perform a detailed analysis of the relationship between measured V_{DR} distributions and relative aggregate device cross sections, it is interesting to note in Fig. 5 that RD03 has a distribution of

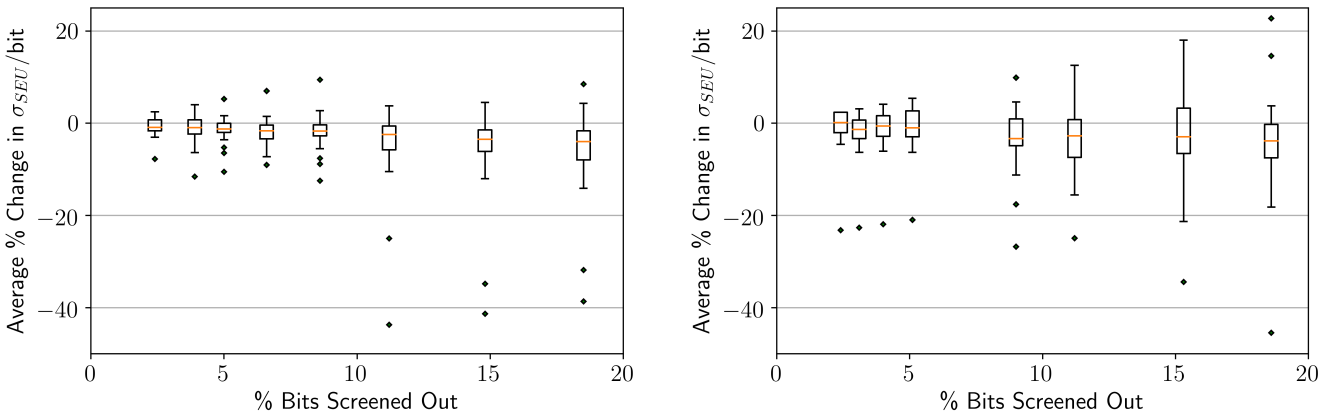

Fig. 10: A plot of the average percentage change in σ_{SEU}/bit as a function of the percentage of cells screened out. RD03 results are shown on left and RD04 on right. In all cases, cells with Q_C values above a certain threshold are kept and all others discarded. This plot is enlarged to show detail in 0-20% of cells screened out range.

measured V_{DR} values that spreads more heavily to the left, into higher V_{DR} values when compared to RD04. Fig. 6 then shows RD03 to have a larger measured cross section than RD04. While more work is needed to confirm this trend, the technique presented in this paper has the potential to identify device variability issues.

VII. Discussion

While other work ([15], [16]) has shown these electrical characterizations to be Gaussian, these data match more closely with modeling predictions done by Wang et. al [29]. Wang et. al's simulation predicted skewed data with a heavy tail toward higher V_{DR} values corresponding to lower Q_C values observed here. One possible such skewed distribution mentioned by Wang et. al is the Weibull distribution, also commonly found in the modeling of LET curves. Should a Weibull distribution be a good fit to these data, the skewed nature of these distributions may, then, be an underlying cause of the observed shape of LET curves.

This work demonstrates that when irradiated by low energy protons, the cells that upset were disproportionately likely to have $Q_C < \overline{Q_C}$. This shift, while statistically significant in likelihood, is relatively small, with the most drastic shift on the order of a 1% smaller mean Q_C from $\overline{Q_C}$. These results show that applying a virtual screen to remove cells identified with the electrical test as having smaller Q_C values than an arbitrary threshold allowed for the σ_{SEU}/bit to be reduced when compared to a baseline of all electrically characterized cells. Fig. 11 shows that as the screening threshold was increased and more cells were removed from the analysis, the cross-section reduced by a greater percentage, although the interquartile range also increased significantly. This increase in the interquartile range is due to performing these calculations on fewer and fewer numbers of upsets ($N - N_T$).

The combination of these results provides strong new evidence that a device does not have a single, constant, σ_{SEU}/bit for low energy particles but rather every cell has a unique σ_{SEU}/bit that when aggregated together becomes the historically reported constant σ_{SEU}.

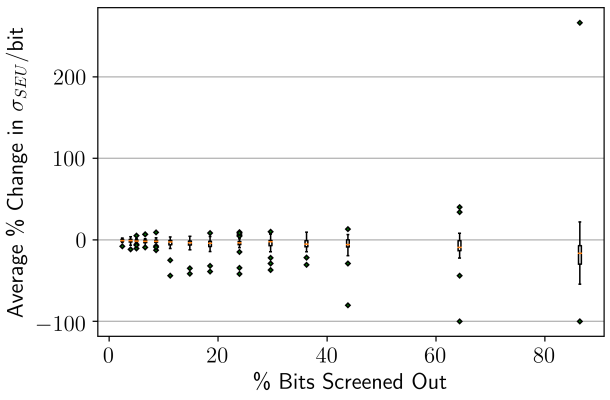

Fig. 11: 15 total screening thresholds applied to RD03 show that, generally, as more bits are screened out the median percent change in the cross section is more negative. However, at the interquartile range that encompasses the middle 50% of trials expands significantly indicating less consistent results.

It is important to realize that these results likely do not extend to particles with LET significantly higher than the threshold. Mitigating the σ_{SEU}/bit is possible only when the charge deposited by a collision is on the order of the real Q_C of a cell. If the charge deposited is well in excess of the highest Q_C of a device, the probability of upset does not vary from cell to cell. This means that the methodology laid out in this paper should not give any information about relative cell susceptibility to ionizing particles with LET much greater than the LET threshold of a device. Rather, this methodology may be useful for mapping out which memory elements will be sensitive at or below a device's $\overline{Q_C}$. This is particularly important for ionizing particles with LET near the LET threshold of the device. Therefore, this technique is not limited to a specific type of particle but is useful for understanding the sensitivity of a device near threshold.

A cell level variation in Q_C implies strongly that there then exists cell level variation in the threshold LET. At the cell level, an LET curve may more closely resemble a step function with a clear minimum particle LET necessary for upset followed by a sharper transition to a saturated cross-section. It could then be the aggregate tendency of devices to contain low Q_C skewed distributions, simulated by [29] and seen in the electrical characterizations presented here, that causes the Wiebull curve seen in standard cross-section data. Then, by appropriately screening out cells with low Q_C, the device-wide threshold LET could be shifted to the right toward higher values, potentially changing the shape of the LET curve to more sharply approach a saturation of the cross-section.

This work has shown that, with a simple electrical test, the cells of an SRAM can be assigned a relative Q_C. Teams developing low-cost CubeSat missions bound for environments dominated by particles with LET near or below a device's threshold LET who do not have access to the resources to perform radiation testing or utilize rad-hardened devices would be able to screen out cells more susceptible to SEUs. This allows a software mitigation to what has always been a hardware issue, potentially leading to fewer CubeSat mission failures, a significant problem in recent years with the CubeSat failure rate being 21% for all missions launched between 2005 and 2018[30]. CubeSats are used here as an example because their low-cost development approach has historically limited their ability to ensure the use of rad-hard devices or to perform independent testing. However, the techniques discussed in this paper are applicable to a wide range of mission designs beyond CubeSats. A further potential application is of "triaged" data storage where temporary data stored in an SRAM device is stored in the cells with the highest Q_C possible at the time of writing.

VIII. Conclusions

This paper presents new evidence that a disproportionate amount of SEUs within an SRAM at low-LET values are due to an increased likelihood of weak cells to upset, rather than a representative sensitive volume within all SRAM cells.

These cells can be screened electrically by mapping relative critical charge values of each cell within an SRAM through a detailed data retention (holding voltage) analysis. This analysis reveals the underlying distribution of cell Q_C variability to be non-Gaussian. Results from low-energy proton irradiation of two COTS SRAM devices show that SEU cross-sections near threshold are dominated by weaker-than-average cells within the DUT (p-values of 7.0E-5 and 3.3E-3 respectively). Furthermore, screening out cells electrically identified as having low Q_C reduced the per bit cross section by an increasing amount as more cells were screened out. At 15% of the weakest cells screened out, the cross-section was reduced by 4% at an approximate LET of 0.12 MeVcm^2/mg. As a result, the error rate can be limited through a device-specific selection of memory cells—presenting a novel software mitigation for the hardware problem of high error rates.

REFERENCES

[1] C. M. Seidleck, K. A. LaBel, A. K. Moran, M. M. Gates, J. M. Barth, E. Stassinopoulos, and T. D. Gruner, "Single Event Effect Flight Data Analysis of Multiple NASA Spacecraft and Experiments; Implications to Spacecraft Electrical Designs," in *Proceedings of the Third European Conference on Radiation and its Effects on Components and Systems*. IEEE, Sep 1995, pp. 581–588.

[2] R. A. Austin, B. D. Sierawski, J. M. Trippe, A. L. Sternberg, K. M. Warren, R. A. Reed, R. A. Weller, R. D. Schrimpf, M. L. Alles, L. W. Massengill *et al.*, "RadFxSat: A Flight Campaign for Recording Single-Event Effects in Commercial Off-the-Shelf Microelectronics," in *2017 17th European Conference on Radiation and Its Effects on Components and Systems (RADECS)*. IEEE, Oct 2017, pp. 19–23.

[3] B. D. Sierawski, R. A. Reed, K. M. Warren, A. L. Sternberg, R. A. Austin, J. M. Trippe, R. A. Weller, M. L. Alles, R. D. Schrimpf, L. W. Massengill *et al.*, "CubeSat: Real-time Soft Error Measurements at Low Earth Orbits," in *2017 IEEE International Reliability Physics Symposium (IRPS)*. IEEE, Apr 2017, pp. 3D–1.1–3D–1.6.

[4] J. Tonfat, F. L. Kastensmidt, L. Artola, G. Hubert, N. H. Medina, N. Added, V. A. Aguiar, F. Aguirre, E. L. Macchione, and M. A. Silveira, "Analyzing the Influence of the Angles of Incidence on SEU and MBU events induced by low LET heavy ions in a 28-nm SRAM-based FPGA," in *2016 16th European Conference on Radiation and Its Effects on Components and Systems (RADECS)*. IEEE, Sep 2016, pp. 1–6.

[5] D. F. Heidel, P. W. Marshall, K. A. LaBel, J. R. Schwank, K. P. Rodbell, M. C. Hakey, M. D. Berg, P. E. Dodd, M. R. Friendlich, A. D. Phan *et al.*, "Low Energy Proton Single-Event-Upset Test Results on 65 nm SOI SRAM," *IEEE Trans. Nucl. Sci.*, vol. 55, no. 6, pp. 3394–3400, Dec 2008.

[6] J. A. Pellish, P. W. Marshall, K. P. Rodbell, M. S. Gordon, K. A. LaBel, J. R. Schwank, N. A. Dodds, C. M. Castaneda, M. D. Berg, H. S. Kim *et al.*, "Criticality of Low-Energy Protons in Single-Event Effects Testing of Highly-Scaled Technologies," *IEEE Trans. Nucl. Sci.*, vol. 61, no. 6, pp. 2896–2903, Dec 2014.

[7] L. W. Massengill, M. L. Alles, S. E. Kerns, and K. L. Jones, "Effects of Process Parameter Distributions and Ion Strike Locations on SEU Cross-Section Data (CMOS SRAMs)," *IEEE Trans. Nucl. Sci.*, vol. 40, no. 6, pp. 1804–1811, Dec 1993.

[8] T. Heijmen and B. Kruseman, "Alpha-particle-induced SER of embedded SRAMs affected by variations in process parameters and by the use of process options," *Solid-State Electronics*, vol. 49, no. 11, pp. 1783 – 1790, Nov 2005.

[9] H. Mostafa, M. H. Anis, and M. Elmasry, "Analytical Soft Error Models Accounting for Die-to-Die and Within-Die Variations in Sub-Threshold SRAM Cells," *IEEE Trans. VLSI Syst.*, vol. 19, no. 2, pp. 182–195, Oct 2011.

[10] A. Griffoni, P. Zuber, P. Dobrovolny, P. J. Roussel, D. Linten, M. L. Alles, R. D. Schrimpf, R. A. Reed, L. W. Massengill, D. Kobayashi, E. Simoen, and G. Groeseneken, "Impact of Process Variability on the Radiation-Induced Soft Error of Nanometer-Scale SRAMs in Hold and Read Conditions," in *2011 12th European Conference on Radiation and Its Effects on Components and Systems*, Sep 2011, pp. 195–201.

[11] A. V. Kauppila, B. L. Bhuva, J. S. Kauppila, L. W. Massengill, and W. T. Holman, "Impact of Process Variations on SRAM Single Event Upsets," *IEEE Trans. Nucl. Sci.*, vol. 58, no. 3, pp. 834–839, Feb 2011.

[12] G. Gasiot, A. Castelnovo, M. Glorieux, F. Abouzeid, S. Clerc, and P. Roche, "Process Variability Effect on Soft Error Rate by Characterization of Large Number of Samples," *IEEE Trans. Nucl. Sci.*, vol. 59, no. 6, pp. 2914–2919, Dec 2012.

[13] J. Yao, Z. Ye, M. Li, Y. Li, R. D. Schrimpf, D. M. Fleetwood, and Y. Wang, "Statistical Analysis of Soft Error Rate in Digital Logic Design Including Process Variations," *IEEE Trans. Nucl. Sci.*, vol. 59, no. 6, pp. 2811–2817, Dec 2012.

[14] D. McMorrow, A. Khachatrian, N. J. . Roche, J. H. Warner, S. P. Buchner, N. Kanyogoro, J. S. Melinger, V. Pouget, C. Larue, A. Hurst, and D. Kagey, "Single-Event Upsets in Substrate-Etched CMOS SOI SRAMs Using Ultraviolet Optical Pulses With Sub-Micrometer Spot Size," *IEEE Trans. Nucl. Sci.*, vol. 60, no. 6, pp. 4184–4191, Dec 2013.

[15] D. Kobayashi, N. Hayashi, K. Hirose, Y. Kakehashi, O. Kawasaki, T. Makino, T. Ohshima, D. Matsuura, Y. Mori, M. Kusano, T. Narita, S. Ishii, and K. Masukawa, "Process Variation Aware Analysis of SRAM SEU Cross Sections Using Data Retention Voltage," *IEEE Trans. Nucl. Sci.*, vol. 66, no. 1, pp. 155–162, Nov 2018.

[16] D. Kobayashi, K. Hirose, K. Sakamoto, S. Okamoto, S. Baba, H. Shindou, O. Kawasaki, T. Makino, T. Ohshima, Y. Mori, D. Matsuura, M. Kusano, T. Narita, and S. Ishii, "Data-Retention-Voltage-Based Analysis of Systematic Variations in SRAM SEU Hardness: A Possible Solution to Synergistic Effects of TID," *IEEE Trans. Nucl. Sci.*, vol. 67, no. 1, pp. 328–335, Nov 2019.

[17] G. Torrens, I. d. Paúl, B. Alorda, S. Bota, and J. Segura, "SRAM Alpha-SER Estimation From Word-Line Voltage Margin Measurements: Design Architecture and Experimental Results," *IEEE Trans. Nucl. Sci.*, vol. 61, no. 4, pp. 1849–1855, May 2014.

[18] D. F. Heidel, P. W. Marshall, J. A. Pellish, K. P. Rodbell, K. A. LaBel, J. R. Schwank, S. E. Rauch, M. C. Hakey, M. D. Berg, C. M. Castaneda *et al.*, "Single-Event Upsets and Multiple-Bit Upsets on a 45 nm SOI SRAM," *IEEE Trans. Nucl. Sci.*, vol. 56, no. 6, pp. 3499–3504, Dec 2009.

[19] T. D. Loveless, M. L. Alles, D. R. Ball, K. M. Warren, and L. W. Massengill, "Parametric Variability Affecting 45 nm SOI SRAM Single Event Upset Cross-Sections," *IEEE Trans. Nucl. Sci.*, vol. 57, no. 6, pp. 3228–3233, Dec 2010.

[20] K. P. Rodbell, D. F. Heidel, H. H. Tang, M. S. Gordon, P. Oldiges, and C. E. Murray, "Low-Energy Proton-Induced Single-Event-Upsets in 65 nm Node, Silicon-on-Insulator, Latches and Memory Cells," *IEEE Trans. Nucl. Sci.*, vol. 54, no. 6, pp. 2474–2479, Dec 2007.

[21] B. D. Sierawski, J. A. Pellish, R. A. Reed, R. D. Schrimpf, K. M. Warren, R. A. Weller, M. H. Mendenhall, J. D. Black, A. D. Tipton, M. A. Xapsos *et al.*, "Impact of Low-Energy Proton Induced Upsets on Test Methods and Rate Predictions," *IEEE Trans. Nucl. Sci.*, vol. 56, no. 6, pp. 3085–3092, Dec 2009.

[22] G. Hubert, S. Duzellier, F. Bezerra, and R. Ecoffet, "MUSCA SEP 3 contributions to investigate the direct ionization proton upset in 65nm technology for space, atmospheric and ground applications," in *2009 European Conference on Radiation and Its Effects on Components and Systems*. IEEE, Sep 2009, pp. 179–186.

[23] E. Cannon, M. Cabanas-Holmen, J. Wert, T. Amort, R. Brees, J. Koehn, B. Meaker, and E. Normand, "Heavy Ion, High-Energy, and Low-Energy Proton SEE Sensitivity of 90-nm RHBD SRAMs," *IEEE Trans. Nucl. Sci.*, vol. 57, no. 6, pp. 3493–3499, Dec 2010.

[24] J. R. Schwank, M. R. Shaneyfelt, V. Ferlet-Cavrois, P. E. Dodd, E. W. Blackmore, J. A. Pellish, K. P. Rodbell, D. F. Heidel, P. W. Marshall, K. A. LaBel *et al.*, "Hardness Assurance Testing for Proton Direct Ionization Effects," *IEEE Trans. Nucl. Sci.*, vol. 59, no. 4, pp. 1197–1202, Jan 2012.

[25] R. K. Lawrence, J. F. Ross, N. F. Haddad, R. A. Reed, and D. R. Albrecht, "Soft Error Sensitivities in 90 nm Bulk CMOS SRAMs," in *2009 IEEE Radiation Effects Data Workshop*. IEEE, Jul 2009, pp. 123–126.

[26] N. F. Haddad, A. T. Kelly, R. K. Lawrence, B. Li, J. C. Rodgers, J. F. Ross, K. M. Warren, R. A. Weller, M. H. Mendenhall, and R. A. Reed, "Incremental Enhancement of SEU Hardened 90 nm CMOS Memory Cell," *IEEE Trans. Nucl. Sci.*, vol. 58, no. 3, pp. 975–980, Apr 2011.

[27] N. Seifert, B. Gill, J. A. Pellish, P. W. Marshall, and K. A. LaBel, "The Susceptibility of 45 and 32 nm Bulk CMOS Latches to Low-Energy Protons," *IEEE Trans. Nucl. Sci.*, vol. 58, no. 6, pp. 2711–2718, Nov 2011.

[28] D. E. Holcomb, W. P. Burleson, and K. Fu, "Power-Up SRAM State as an Identifying Fingerprint and Source of True Random Numbers," *IEEE Trans. Comput.*, vol. 58, no. 9, pp. 1198–1210, Nov 2008.

[29] J. Wang, A. Singhee, R. A. Rutenbar, and B. H. Calhoun, "Two Fast Methods for Estimating the Minimum Standby Supply Voltage for Large SRAMs," *IEEE Trans. Comput.-Aided Design Integr. Circuits Syst.*, vol. 29, no. 12, pp. 1908–1920, Nov 2010.

[30] T. Villela, C. A. Costa, A. M. Brandão, F. T. Bueno, and R. Leonardi, "Towards the Thousandth CubeSat: A Statistical Overview," *International Journal of Aerospace Engineering*, vol. 2019, Article ID 5063145, Jan 2019.